A Non-periodic Planning and Control Framework of Dynamic Legged Locomotion

Ye Zhao
Assistant Professor*
G.W.Woodruff School of Mechanical Engineering
Georgia Institute of Technology
Atlanta, Georgia 30313
Email: ye.zhao@me.gatech.edu

Yan Gu
Assistant Professor
The Department of Mechanical Engineering
University of Massachusetts Lowell
Lowell, MA 01854
Email: yan_gu@uml.edu

Abstract: This study proposes an integrated planning and control framework for achieving three-dimensional robust and dynamic legged locomotion over uneven terrain. The proposed framework is composed of three hierarchical layers. The high-level layer is a state-space motion planner designing highly dynamic locomotion behaviors based on a reduced-order robot model. This motion planner incorporates two robust bundles, named as invariant and recoverability bundles, which quantify analytical state-space deviations for robust planning design. The low-level layer is a model-based trajectory tracking controller capable of robustly realizing the planned locomotion behaviors. This controller is synthesized based on full-order hybrid dynamic modeling, model-based state feedback control, and Lyapunov stability analysis. The planning and control layers are concatenated by a middle-level trajectory generator that produces nominal behaviors for a full-order robot model. The proposed framework is validated through flat and uneven terrain walking simulations of a three-dimensional bipedal robot.

1 Introduction

Achieving robust and dynamic legged locomotion in complex environments becomes imperative for numerous real-world robotic applications such as search and rescue operations, disaster response, and supply delivery. Although planning and control for robust and dynamic locomotion has been extensively investigated during the past few decades, it is still a fundamentally challenging problem. Typically, in the legged locomotion community, planning and control problems are handled separately, which greatly limits the overall locomotion performance and achievable formal guarantees. For instance, motion planning approaches [1, 2] often ignore stabilization and trajectory tracking capabilities of the underlying controllers, leaving the control systems lack of formal guarantees on stability as well as robustness to external disturbance and model uncertainties. Meanwhile, although various locomotion control approaches, such as the Hybrid-Zero-Dynamics (HZD) framework [3,4,5,6,7], have realized provable stabilization, it remains an open problem to seamlessly integrate these controllers with high-level task and motion planners.

A typical approach of integrated planning and control is to use a reduced-order dynamic model at the high-level motion planner while leaving the full-order robot model to be handled by the low-level controller [8,9,**?**]. Using a reduced-order model (e.g., prismatic inverted pendulum model [10] or a centroidal momentum model [11]) significantly reduces the computational burden, allowing for efficient and multi-task motion planning. Meanwhile, a full-order model accurately captures whole-body dynamics, and thus enables controller design that achieves significantly higher legged locomotion performance [5] than a reduced-order model based controller design [12]. Despite significant progress in simultaneously reasoning locomotion planning and control, existing approaches tend to assume that the low-level control can always successfully track desired trajectories designed by the high-level planner [13, 14], which is often violated in the presence of external disturbance and model uncertainties and thus lacks formal guarantees on robustness.

Providing formal robustness guarantee through integrated planning and control is essential to achieving robust and dynamic legged locomotion in complex environments. It

*The two authors are equally contributed.

is difficult to provide formal guarantees on the robust performance of a locomotion system that exploits different models for planning and control. If this difficulty is overcome properly, an integrated planning and control framework can potentially scale up to a high-dimensional space while maintaining formal guarantees on robustness.

The objective of this work is to take an initial step towards a seamlessly integrated planning and control framework that can provably achieve robust and dynamic locomotion behaviors over uneven terrain. The pivotal components of this framework include: (i) a motion planner that uses reduced-order dynamic modeling and generates non-periodic nominal motions; (ii) a hybrid automaton that guides the high-level planning sequence; (iii) invariant and recoverability bundles that characterize center-of-mass state-space robustness for high-level re-planning; (iv) a trajectory generator that produces full-dimensional nominal trajectories based on full-order modeling; and (v) a feedback controller that uses full-order dynamic modeling and can provably guarantee reliable trajectory tracking.

The main contributions of this study are summarized as follows.

- Designing a robust, non-periodic state-space planner capable of generating dynamic three-dimensional non-periodic locomotion behaviors. Compared to other reduced-model-based locomotion planners, we have a large focus on the generation of non-periodic gait over uneven terrains and under external disturbances.
- Proposing robustness metrics in the motion planner and a re-planning mechanism to deal with disturbances: (i) the motion planner devises an analytical robust metric to characterize state-space deviations; and (ii) a feedback mechanism sends full-order joint states from the low-level controller to the motion planner for trajectory re-planning when a large external disturbance perturbs the state out of the robust bundles defined in (i).
- Providing formal controller design. A trajectory tracking controller is introduced to provably achieve reliable tracking of non-periodic trajectories generated by the high-level motion planner. To the best of the authors' knowledge, it is the first time that provably reliable tracking of non-periodic trajectories over uneven terrains is realized.
- Designing a middle-layer trajectory generator to seamlessly integrate high-level motion planner and low-level controller.

This paper is organized as follows: Related work is elaborated in Section 2. A reduced-order of bipedal locomotion is presented in Section 3. Section 4 introduces robust bundles and a hybrid automaton that governs an overall locomotion planning process. In Section 5, a trajectory tracking controller is proposed based on full-order dynamic modeling, input-output linearization, and formal stability analysis. Section 6 introduces a trajectory generation method to build the connection between the high-level planner and low-level controller layers. Simulation results are shown in Section 7. This paper ends with discussions and conclusions in Sections 8-9.

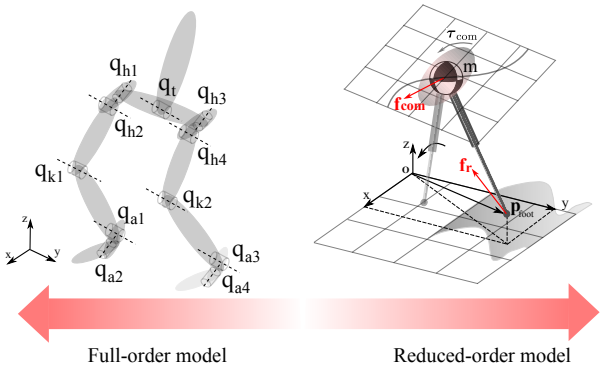

Fig. 1: A full-order model of a biped with nine revolute joints (left) and a reduced-order model with Center of Mass (CoM) motion constrained to a varying-height, piecewise-linear 3D surface (right).

2 Related Work

Simplified locomotion models: Numerous center-of-mass (CoM) trajectory design methods for dynamic locomotion have been proposed over the past few decades. The Capture Point method [15] and Divergent Component of Motion [16] presented general three-dimensional locomotion frameworks. However, a common shortcoming of these approaches lies in over-constraining the models and center-of-mass (CoM) motions, for instance, a common assumption on a constant CoM height as shown in the linear inverted pendulum model. A tangible benefit of such an assumption is the existence of closed-form solutions of the robot model further facilitating the use of linear control analysis and synthesis methods. However, leveraging these models to rough terrain locomotion becomes limited. How to relax conservative model assumptions to target rough terrain maneuvering becomes imperative. To relax this assumption, a variety of extended work has been investigated recent years. For instance, [17] allowed the CoM to move within a non-constant height 3D plane. Designing CoM trajectories with varying heights was also studied in [16, 18]. The work in [19] proposed a nonlinear inverted pendulum model where the CoM path is extended to a parabola, but it focuses on planar locomotion, and the induced nonlinearities eliminate appealing linear system properties. In contrast to these previous studies, our work allows the CoM to stay within a parametric 3D surface such that the framework is applicable to rough terrain locomotion while maintaining the favorable linear system properties.

Robustness reasoning in motion planning: The concept of robust hybrid automaton was introduced in [20] to achieve time-optimal motion planning of a helicopter in an environment with obstacles. The same group studied robustness to model uncertainties [21] but ignored large external disturbances. Lately, [22] extended this line of research to accommodate external disturbances (e.g., cross-wind) by computing funnels via Lyapunov functions and switching among them for maneuvering unmanned air vehicles. Regarding the natural hybrid property of legged locomotion, we propose to

develop a hybrid automaton algorithm that robustly switches among different contact modes and govern the whole planning process. Another significant feature of our work is that we design a state-space re-planning strategy at run-time while the previous works merely rely on pre-defined motion primitives.

Provable walking stabilization: Provably stable bipedal robotic walking was first realized through the HZD framework [3, 23, 24], which stabilizes legged locomotion by orbitally stabilizing the control system. To realize non-periodic locomotion, the concept of gait library has been introduced within the HZD framework [6], and velocity tracking in Cartesian space has been investigated based on the Partial-Hybrid-Zero-Dynamics (PHZD) framework [4]. Because orbitally stabilizing control drives a robot's state to a periodic orbit (or curve) in the state space instead of a specific time trajectory residing in the orbit, it cannot realize reliable tracking of time-varying trajectories, which, however, is often required in practical robotic applications. Indeed, trajectory tracking control of hybrid systems that include legged robots is an active research area. Previous studies have investigated Lyapunov-based controller design methods for provably solving the tracking problem [25, 26, 27, 28, 29]. However, it is not clear how these methods could be used to explicitly inform the design of tracking controllers for legged locomotion systems. Thus, we propose a low-level controller based on Lyapunov stability analysis for provably solving the control problem of tracking time-varying trajectories.

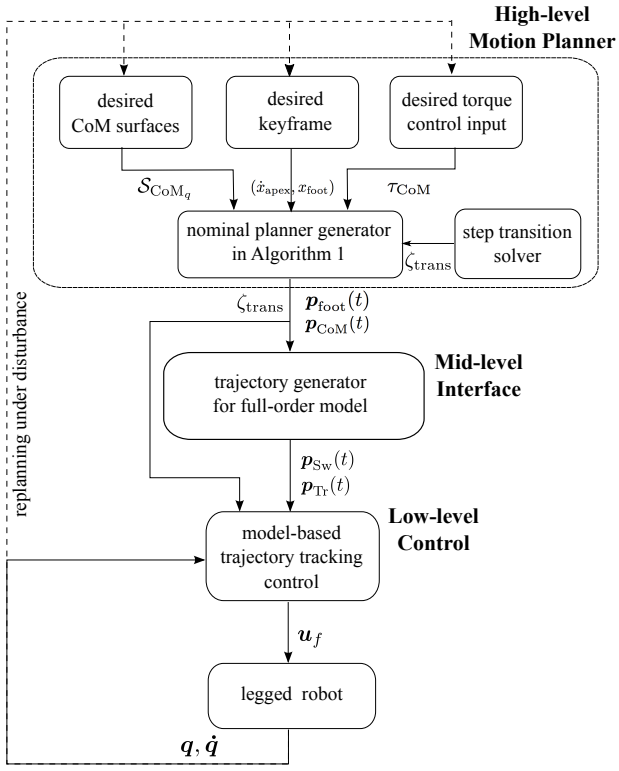

Fig. 2: Hierarchical planning and control framework. This framework is composed of the high-level state-space planner and the low-level trajectory tracking controller. There exists a middle layer for generating nominal trajectories for the full-order model, dubbed as "trajectory generator for full-order model". The high-level planner sends nominal CoM trajectories $p_{\mathrm{CoM}}(t)$, foot placements p_{foot}, and landing instants ζ_{trans} to the low-level controller. After the middle layer, the controller computes joint torque commands sent to the robot. The feedback loop sends the robot measured states to the low-level controller. These measured states are only sent to the high-level planner for the re-planning strategy whenever necessary, i.e., when a disturbance is detected.

3 Non-periodic Motion Planning

This section presents a reduced-order bipedal walking model designed for phase-space locomotion planning. A salient feature of this model is to allow non-periodic locomotion and non-constant-height center-of-mass (CoM) surface design.

3.1 Reduced-order model

Reduced-order models have been extensively used in legged locomotion planning due to its tractable computation effort and convenient walking trajectory design [30] [31] [32]. As observed by studies in human dynamic locomotion [33], a bipedal walking robot resembles an inverted pendulum model (see the right subfigure in Fig. 1). A bipedal walking robot can behave as an inverted pendulum under the assumptions of massless legs and whole-body mass concentrated at the hip position. We propose a reduced-order model named as Prismatic Inverted Pendulum Model (PIPM), suitable for non-periodic walking. In this model, a biped's position is typically represented by its 3D center-of-mass (CoM) position $p_{\mathrm{CoM}} = (x_{\mathrm{CoM}}, y_{\mathrm{CoM}}, z_{\mathrm{CoM}})^T$. Numerous human walking [34] and balancing [35] results emphasize that controlling the centroidal angular momentum improves CoM tracking, balancing and recovering from disturbances. During a single-support phase, the sum of moments with respect to the global reference frame is

$$-p_{\mathrm{foot}} \times f_r + p_{\mathrm{CoM}} \times \Big(f_{\mathrm{CoM}} + mg\Big) + \tau_{\mathrm{CoM}} = 0, \qquad (1)$$

where $p_{\mathrm{foot}} = (x_{\mathrm{foot}}, y_{\mathrm{foot}}, z_{\mathrm{foot}})^T$ is the support foot position, $f_r \in \mathbb{R}^3$ is the ground-reaction force, $f_{\mathrm{CoM}} \in \mathbb{R}^3$ is the center-of-mass inertial force, m is the whole-body mass, $g = (0, 0, -9.8)^T \in \mathbb{R}^3$ is the gravitational acceleration, and $\tau_{\mathrm{CoM}} = (\tau_x, \tau_y, \tau_z)^T$ is the whole-body inertial torque about the CoM. The system's linear force equilibrium are formulated as $f_r = f_{\mathrm{CoM}} + mg$, allowing us to simplify Eq. (1) to the following general PIPM equation

$$\Big(p_{\mathrm{CoM}} - p_{\mathrm{foot}}\Big) \times (f_{\mathrm{CoM}} + mg) = -\tau_{\mathrm{CoM}}. \qquad (2)$$

For our purposes, we consider a class of prismatic inverted pendulums whose CoM is restricted to a 3D non-constant-height path surface, as summarized below.

Assumption 1. *The CoM motion of the inverted pendulum model is constrained within piece-wise linear 3D planes (i.e., path surfaces). During the k^{th} step, the linear CoM path*

surface $\mathcal{S}_{\text{CoM}_k}$ is defined as

$$\mathcal{S}_{\text{CoM}_k} = \{p_{\text{CoM}_k} | z_{\text{CoM}} - a_k x_{\text{CoM}} - b_k y_{\text{CoM}} - c_k = 0\}, \quad (3)$$

where a_k and b_k are slope coefficients of the linear CoM path surfaces that we design while c_k is a constant coefficient of this surface.

Let $x_r = (p_{\text{CoM}}^T, \dot{p}_{\text{CoM}}^T)^T \in \mathcal{X}_r \subseteq \mathbb{R}^6$ be the state-space vector, where $\mathcal{X}_r$ is a compact set of admissible CoM positions and velocities. Based on Assumption 1, the general PIPM model during the k^{th} walking step $\dot{x}_r = \mathcal{F}(k, x_r, u_r)$ is simplified to the state-space equations with three-dimensional accelerations

$$\begin{pmatrix} \ddot{x}_{\text{CoM}} \\ \ddot{y}_{\text{CoM}} \\ \ddot{z}_{\text{CoM}} \end{pmatrix} = \begin{pmatrix} \underbrace{\omega_k^2(x_{\text{CoM}} - x_{\text{foot}_k}) - \frac{\omega_k^2}{mg}(\tau_y + b_k \tau_z)}_{A_x} \\ \underbrace{\omega_k^2(y_{\text{CoM}} - y_{\text{foot}_k}) - \frac{\omega_k^2}{mg}(\tau_x + a_k \tau_z)}_{A_y} \\ a_k A_x + b_k A_y \end{pmatrix}, \quad (4)$$

where $u_r = (\omega_k, \tau_{\text{CoM}_k}, p_{\text{foot}_k})^T \in \mathcal{U}_r$ represents the input variables ($\mathcal{U}_r$ is a compact set of admissible inputs); the subscript "r" denotes "reduced-order". $\mathcal{F}$ represents a vector field of inverted pendulum dynamics, which, given fixed input u_r, is assumed to be infinitely continuous and differentiable in the domain $\mathcal{D}(q_k)$ and globally Lipschitz in $\mathcal{X}_r$, where q_k indicates the locomotion mode of k^{th} walking step. The slope of locomotion state-space asymptotic ω_k is a control parameter defined as

$$\omega_k = \sqrt{\frac{g}{z_{\text{apex}_k}}}, \quad (5)$$

where $z_{\text{apex}_k} = (a_k x_{\text{foot}_k} + b_k y_{\text{foot}_k} + c_k - z_{\text{foot}_k})$ corresponds to the vertical distance between the CoM and the location of the foot contact at the instant when the CoM is on the top of the foot location. Note that this reduced-order model only presents continuous dynamics. We will handle the discrete impact dynamics in the full-order model for the controller design.

3.2 Non-periodic state-space motion planner

Let us focus on the robot's sagittal walking dynamics, and the state vector x_r is simplified as $\{x_{\text{CoM}}, \dot{x}_{\text{CoM}}\}$. This system has control inputs $u_{r,x} = (\omega, \tau_y, \tau_z, x_{\text{foot}}, z_{\text{foot}})^T$, where the subscript 'k' is ignored for brevity. As we are previously motivated, the path manifold $\mathcal{S}_{\text{CoM}}$ is defined a priori conforming to contact terrains. By Eq. (5), once the path manifold is defined for given contact locations, the set of state-space asymptotic slopes ω is also known from Eq. (5). Accordingly, we design the following algorithm to produce nominal state-space trajectories of the robot's center-of-mass in the sagittal direction:

Algorithm 1. Nominal non-periodic motion planner.

Input:
(i): $\mathcal{S}_{\text{CoM}} \leftarrow \{\mathcal{S}_{\text{CoM}_k} : [\zeta_{k-1}, \zeta_k] \rightarrow \mathbb{R}^3, \forall k \in \{1, \ldots, N\}$
(ii): $x_{\text{foot}} \leftarrow \{x_{\text{foot}_1}, x_{\text{foot}_2}, \ldots, x_{\text{foot}_N}\}$
(iii): $z_{\text{foot}} \leftarrow \{z_{\text{foot}_1}, z_{\text{foot}_2}, \ldots, z_{\text{foot}_N}\}$
(iv): $\dot{x}_{\text{apex}} \leftarrow \{\dot{x}_{\text{apex}_1}, \dot{x}_{\text{apex}_2}, \ldots, \dot{x}_{\text{apex}_N}\}$
(v): $(\tau_y(t), \tau_z(t)) \leftarrow 0$
Operation:
(i): $\omega := \{\omega_1, \omega_2, \ldots, \omega_N\}$ is assigned via Eqs. (5)
(ii): $(x_{\text{CoM}}(t), \dot{x}_{\text{CoM}}(t), \ddot{x}_{\text{CoM}}(t))$ via Eq. (4)
Output:
State-space trajectories $\mathcal{M}_{\text{CoM}} := \bigcup_k \mathcal{M}_{\text{CoM}_k}$

In this algorithm, $\dot{x}_{\text{apex}}$ represents the desired CoM apex velocity. It is worthy noting that the desired CoM surfaces, nominal foot positions, keyframe states, and zero torso torques are provided a priori by the designer or high-level task planning algorithms [36]. Although foot positions are given as input, our planning method can handle terrain uncertainties via robust concepts proposed in the next subsection. For dynamic legged robots, knowing accurate terrain information is unrealistic. Nevertheless, estimating the terrain geometry to certain extent is practically plausible. Therefore, we build robust bundles around the nominal trajectories to quantify local state deviations caused by terrain uncertainties. Accordingly, the torso torque control input will be non-zero. Considering the equivalence of sagittal and lateral dynamics in Eq. (4), a similar algorithm can be designed for lateral CoM trajectory generation. Compared with other existing locomotion frameworks, a salient feature of our algorithm is to allow non-periodic gait generation and the ease of accomplishing complex locomotion behaviors via the keyframe state design. In addition, only the CoM surface is provided as input, and the actual CoM trajectory needs to be solved based on the PIPM dynamics in Eq. (4). The end-to-end locomotion planning process is shown in Fig. 2.

4 Robust Hybrid Locomotion Planning

Legged locomotion naturally exhibits hybrid dynamics. In this section, we will propose a hybrid automaton to model the hybrid process of bipedal walking as well as to propose robustness concepts in the CoM state space. The hybrid automaton serves as a core formulation throughout our integrated planning and control framework while governing (i) the state-space planner in Section 3 and (ii) a robust replanning strategy to be introduced in Section 4).

We assign each walking step as a mode in finite state machine (FSM), i.e., $q_i \in \mathcal{Q} = \{q_1, q_2, ..., q_{n_d}\}$, where n_d represents the number of FSM states. For bipedal robot walking, we encode two modes: left foot contact q_l and right foot contact q_r (i.e., $\mathcal{Q} = \{q_l, q_r\}$). On each mode q, we have the state variables, $x_r \in \mathcal{X}_r$. The region of the state-space that belongs to each mode q_i is defined by domain $\mathcal{D}(\cdot)$. Thus $\mathcal{D}(q) : \mathcal{Q} \rightarrow 2^{\mathcal{X}_r}$, where $2^{\mathcal{X}_r}$ represents the power set

(all the subsets) of $\mathcal{X}_r$. For each mode, the governing continuous dynamics equation is defined as $\dot{x}_r = \mathcal{F}(q, x_r, u_r, w)$. $u_r \in \mathcal{U}_r \subseteq \mathbb{R}^m$ is the control vector, and $w \in \mathcal{W} \subseteq \mathbb{R}^{n_{\text{dist}}}$ is the disturbance vector. The state of the hybrid system consists of both continuous and discrete states, $s = (q, x_r) \in \mathcal{S}$, where $\mathcal{S} : \mathcal{Q} \times \mathcal{X}_r$ is the hybrid automaton state space. The initial condition is defined by $s_0 = (q_0, x_{r,0}) \in I : \mathcal{Q} \times \mathcal{X}_r$.

We represent the hybrid system as a directed graph $(\mathcal{Q}, \mathcal{E})$. The *nodes* are represented by $q \in \mathcal{Q}$, the *edge* $\mathcal{E}_{i,j} = \mathcal{E}(q_i, q_j) \in \mathcal{E} : \mathcal{Q} \times \mathcal{Q}$, and the *transition* is represented by $q_i \to q_j$. The condition that triggers the discrete event (i.e., switch or jump) is determined by the *guard* in hybrid systems. The guard $\mathcal{G}_{i,j} = \mathcal{G}(q_i, q_j) \coloneqq \{(q_i, q_j) \in \mathcal{Q} \times \mathcal{Q} \to 2^{\mathcal{X}_r}\}$. The state, input, or their vector fields change discontinuously after the transition.

Given an initial condition $(\zeta_0, q_i, x_r(\zeta_0)) \in I \setminus \mathcal{G}(q_i, q_j)$ ("$\setminus$" represents set difference), the continuous state x_{r,q_i} evolves within domain $\mathcal{D}(q_i)$ where the discrete state q remains q_i. x_{r,q_i} evolves till hitting $\mathcal{G}(q_i, q_j)$ of $\mathcal{E}(q_i, q_j)$. Then the discrete state switches from q_i to q_j while x_{r,q_i} is reset.After this reset, continuous state evolves till next step transition occurs. Now let us formulate a robust hybrid automaton for the locomotion process. This robust hybrid automaton is inspired by the work of [37, 20, 38] and defined as below.

Definition 1. *A phase-space robust hybrid automaton $\mathcal{H}_{\text{PSP}}$ is a dynamical system, described by a n-tuple*

$$\mathcal{H}_{\text{PSP}} = (\mathcal{Q}, \mathcal{X}_r, \Sigma, \mathcal{W}, \mathcal{U}_r, I, \mathcal{D}, \mathcal{R}, \mathcal{B}, \mathcal{E}, \mathcal{G}, \mathcal{T}). \quad (6)$$

The tuple components of this robust hybrid automaton are defined in Appendix A, and in particular, the robust bundles $\mathcal{R}$ and $\mathcal{B}$ will be introduced below. To the best of authors' knowledge, we are among the first to propose robust hybrid automaton for legged locomotion. Despite specific robot dynamics, this automaton is extendable to a broader class of legged robots.

4.1 Robust bundles

The proposed hybrid automaton in Definition 1 incorporates two state-space robust bundles: an *invariant set* $\mathcal{B}(\varepsilon)$ and a *recoverability set* $\mathcal{R}$. The concept of robustness in this study refers to CoM trajectory disturbance rejection. Namely, given a state disturbance, the planner designs a control strategy to recover the CoM state to the nominal trajectory. Again taking sagittal dynamics for instance, we define the robust bundles as:

Definition 2 (Invariant Bundle)**.** *A bundle $\mathcal{B}(x_{r,\zeta_0}, \varepsilon)$ is an* invariant bundle *if*

$$\forall x_{r,0} \in \mathcal{B}(x_{r,\zeta_0}, \varepsilon),\ \varepsilon > 0,\ x_{r,\zeta_0} \subseteq \mathcal{X},\ \zeta_0 \in \mathbb{R}_{\geq 0} \quad (7)$$

$x_{r,\zeta}$ satisfies:

$$x_{r,\zeta} \in \mathcal{B}(x_{r,\zeta_0}, \varepsilon) \quad \forall\, \zeta \geq \zeta_0, \quad (8)$$

where, ζ_0 and ζ are initial and current phase progression variables, respectively. x_{r,ζ_0} is an initial condition.

Definition 3 (Finite Phase Recoverability Bundle)**.** *The bundle $\mathcal{B}(x_{r,0}, \varepsilon)$ around a CoM state-space manifold has a* finite phase recoverability bundle*, $\mathcal{R}(\mathcal{B}(x_{r,0}, \varepsilon), \rho)$, for which there exists a finite phase progression variable increment $\bar{\zeta} > 0$ such that $\forall x_{r,\zeta_0} \in \mathcal{R}$, $x_{r,\zeta}$ will recover to the invariant bundle after $\zeta_0 + \bar{\zeta}$ but before the final instant ζ_f,*

$$\mathcal{R}(\mathcal{B}(x_{r,0}, \varepsilon), \rho) = \big\{ \exists\, \gamma \geq \rho \geq \varepsilon,\ \bar{\zeta} > 0 \,\big|\, \forall x_{r,\zeta_0} \in \mathcal{B}_i(x_{r,0}, \gamma) \\ \to x_{r,\zeta} \in \mathcal{B}(x_{r,0}, \varepsilon)\ \forall \zeta_0 + \bar{\zeta} \leq \zeta \leq \zeta_f \big\}$$

Note that a control input needs to be designed for the recoverability bundle in Def. 3. For general dynamical systems, it is challenging to compute exact solutions of these two sets due to nonlinear system dynamics. Our study uses the PIPM model in Eq. (4) to define the two robust bundles above. In the simulation section, we will demonstrate how to use these robust bundles to achieve robust re-planning when disturbance occurs. In the next section, we will design an input-output linearizing controller at the low-level for achieving robust trajectory tracking. In this study, we mainly study the disturbance from initial state deviations and external impulse perturbations on CoM states.

The non-periodic locomotion process can be characterized by a keyframe map as below.

Definition 4 (Non-Periodic Keyframe Mapping)**.** *We define a keyframe map of non-periodic gaits as a return map Φ that takes the robot's center-of-mass state from one desired keyframe $(\dot{x}_{\text{apex}_q}, x_{\text{foot}_q})$ to the next one, and via the control input $u_{r,x}$ i.e.*

$$(\dot{x}_{\text{apex}_{q+1}}, x_{\text{foot}_{q+1}}) = \Phi(\dot{x}_{\text{apex}_q}, x_{\text{foot}_q}, u_{r,x}). \quad (9)$$

The CoM apex states represent key states for agile walking. For instance, users can design "non-periodic" keyframes that regulate the walking speed and steer the robot through its walk. For this study, we design keyframes according to the terrain geometries and locomotion tasks.

4.2 Robust re-planning strategy

This subsection presents our re-planning strategy in response to external disturbances. Formal design of re-planning strategies can be referred to the work [32]. When an external sagittal disturbance is exerted on the robot's trunk, we detect whether the CoM state is perturbed outside the recoverability bundle at run-time. If this situation occurs, multiple strategies can be used to re-plan CoM trajectories,

such as redesigning keyframe states (i.e., next foot placement and sagittal apex velocity), CoM surfaces, contact switching instants, or a combination of them. In this study, the re-planning horizon is chosen as one walking step unless otherwise specified. It is noteworthy that all these strategies are applicable to multi-step horizon. The re-planning principle relies on two main factors: (i) allowable control authority, and (ii) the direction, magnitude, and occurrence instant of the disturbance. In addition, the planner can handle other types of disturbances including lateral CoM disturbance, terrain height uncertainties, and swing-foot disturbance.

5 Controller Design Based on a Full-Order Model

To achieve reliable trajectory tracking control for a fully actuated bipedal robot, this section presents our proposed controller design based on full-order dynamic modeling and Lyapunov stability analysis.

5.1 Full-order dynamic modeling

A full-order model serves as a basis of controller design in this study. Because a full-order model accurately captures a robot's complete dynamic behaviors for all degrees of freedom (DoFs) involved in walking, the controller designed to achieve reliable trajectory tracking will also be valid for the actual robot. The following assumption is made in full-order dynamic modeling [5, 39]:

Assumption 2. *a) All joints of the robot are independently actuated. b) During single-support modes, the support foot remains a static, full contact with the ground , i.e., no foot slipping or rolling occurs. c) The swing-foot landing impact is modeled as an impact between rigid bodies. d) Double-support modes are instantaneous.*

Assumption 2 indicates that the bipedal robot considered in this study is fully actuated during continuous modes. Its full-order dynamics during a continuous mode can be expressed as [3]

$$M(\theta)\ddot{\theta} + c(\theta,\dot{\theta}) = Bu_f, \tag{10}$$

where the subscript "f" denotes "full-order", $\theta \in \Theta_f \subset \mathbb{R}^n$ is the joint-position vector, $u_f \in \mathcal{U}_f \subset \mathbb{R}^m$ is the joint-torque vector, $M : \Theta_f \to \mathbb{R}^{n\times n}$ is the inertia matrix, $c : \mathcal{T}\Theta_f \to \mathbb{R}^n$ is the sum of the Coriolis, centrifugal, and gravitational terms, and $B \in \mathbb{R}^{n\times m}$ is a nonsingular input matrix. Here, Θ_f is the configuration space, $\mathcal{T}\Theta_f$ is the tangential space of Θ_f, and $\mathcal{U}_f$ is a compact set of admissible joint torques. $m = n$ due to full actuation. The impact dynamics can be expressed as:

$$\begin{bmatrix}\theta^+\\ \dot{\theta}^+\end{bmatrix} = \Delta_f(\theta^-,\dot{\theta}^-), \tag{11}$$

where $\Delta_f : \mathcal{T}\Theta_f \to \mathbb{R}^{2n}$. The guard representing the state-triggered discrete event of a swing-foot landing can be expressed as

$$\mathcal{G}_f(\theta,\dot{\theta}) := \{(\theta,\dot{\theta}) \in \mathcal{T}\Theta_f : z_{sw}(\theta) = 0, \dot{z}_{sw}(\theta,\dot{\theta}) < 0\},$$

where $z_{sw}(\theta)$ is the swing-foot height above the ground.

5.2 Model-based trajectory tracking control

The control objective of this study is to achieve provably reliable tracking of the nominal trajectories. Note that stable walking refers to walking without falling and is guaranteed if the closed-loop control system is stable.

The variables of interest include: (i) the CoM position for following the nominal CoM path; (ii) the swing-foot position for avoiding collision with the ground during swinging and reaching the nominal touchdown position; and (iii) the swing-f and the trunk angle for maintaining an upright posture. The nominal trajectories of these variables are often planned as explicit functions of time in real-world robotic applications. In this study, the nominal CoM and swing-foot touchdown positions are planned by the state-space planner in Section 3, while the nominal foot swinging and trunk trajectories are planned by a trajectory generator to be introduced in Section 6.

Designing a trajectory tracking controller for a bipedal walking robot is complicated due to its hybrid, nonlinear dynamics and the time-varying nature of the nominal trajectories. To simplify the controller design, input-output linearization [40] is first utilized to linearize the nonlinear continuous-mode dynamics in Eq. (10).

Let h denote the trajectory tracking error, which is defined in Section 6. Suppose that the inertia matrix M and $\frac{\partial h}{\partial q}M^{-1}B$ are both invertible on Θ_f [3]. Then, with h chosen as the output function y, i.e., $y = h$, the proposed input-output linearizing controller design can be expressed as

$$u_f = (\tfrac{\partial h}{\partial \theta}M^{-1}B)^{-1}(v + \tfrac{\partial h}{\partial \theta}M^{-1}c - \tfrac{\partial^2 h}{\partial t^2} - \tfrac{\partial}{\partial \theta}(\tfrac{\partial h}{\partial \theta}\dot{\theta})\dot{\theta}).$$

With v chosen as a proportional-derivative (PD) control law, i.e., $v = -K_P y - K_D \dot{y}$, where $K_P \in \mathbb{R}^{m\times m}$ and $K_D \in \mathbb{R}^{m\times m}$ are positive-definite diagonal matrices, the continuous-mode closed-loop dynamics become $\ddot{y} = -K_P y - K_D \dot{y}$. Defining $x_f := \left[y^T,\ \dot{y}^T\right]^T$, one can compactly express the closed-loop dynamics as:

$$\Sigma_f : \begin{cases} \dot{x}_f = Ax_f, & \text{if } (t,x_f^-) \notin \mathcal{G}_{f,x}(t,x_f);\\ x_f^+ = \Delta_{f,x}(t,x_f^-), & \text{if } (t,x_f^-) \in \mathcal{G}_{f,x}(t,x_f); \end{cases} \tag{12}$$

where $A := \begin{bmatrix} 0 & I \\ -K_P & -K_D \end{bmatrix}$ ($0 \in \mathbb{R}^{m\times m}$ is a zero matrix and $I \in \mathbb{R}^{m\times m}$ is an identity matrix) and the expressions of $\mathcal{G}_{f,x}$ and $\Delta_{f,x}$ can be obtained from $\mathcal{G}_f$, Δ_f, and y. Note that $\mathcal{G}_{f,x}$ and $\Delta_{f,x}$ are explicitly time-dependent because the trajectory tracking error h is explicitly time-dependent.

Thanks to full actuation during continuous modes, the trajectory tracking error h can be exponentially driven to zero within continuous modes if the PD gains K_P and K_D are properly chosen. However, the discrete impact dynamics cannot be directly controlled due to the infinitesimal duration of a foot-landing impact, leaving the nonlinear, time-varying closed-loop reset map in Eq. (12) uncontrolled. It is then necessary to formally analyze the stability of the overall hybrid closed-loop system for deriving sufficient conditions under which the proposed continuous-mode control law can provably guarantee reliable trajectory tracking.

5.3 Closed-loop stability analysis

In this subsection, we utilize multiple Lyapunov analysis to construct closed-loop stability conditions for the hybrid, nonlinear, time-varying system in Eq. (12) [41, 42].

Analyzing the stability of the closed-loop system in Eq. (12) is theoretically difficult due to two reasons. First, the closed-loop reset map is highly complex, which is uncontrolled, time-varying, and highly nonlinear. Second, there is always a mismatch between the actual and the nominal impact times because the foot-landing event is state-triggered rather than fixed-time [27, 29]. Hence, to establish the closed-loop stability conditions, the effects of both the reset map and the impact-time mismatch on the evolution of a Lyapunov function candidate should be explicitly analyzed, leading to complex stability analysis.

According to the stability analysis via the construction of multiple Lyapunov functions [43], the hybrid time-varying system in Eq. (12) is exponentially stable if there exists a positive number d such that (i) $V(x_f)$ is exponentially decreasing during each continuous mode and that (ii) the sequence $\{V|_1^+, V|_2^+, V|_3^+ ...\}$ strictly decreases for any $x_f(0^+) \in B_d(0) := \{x_f : \|x_f\| \leq d\}$.

Suppose the PD gains K_P and K_D are chosen such that the matrix A in Eq. (12) is Hurwitz. Then, there exists a Lyapunov function candidate $V(x_f)$ and positive constants c_1, c_2, and c_3 such that $V(x_f)$ satisfies

$$c_1||x_f||^2 \leq V(x_f) \leq c_2||x_f||^2 \text{ and } \dot{V}(x_f) \leq -c_3 V(x_f) \quad (13)$$

for all x_f during any continuous mode [40].

Let T_k denote the k^{th} actual impact instant. In the following stability analysis, $\star(T_k^-)$ and $\star(T_k^+)$ will be denoted as $\star|_k^-$ and $\star|_k^+$, respectively, as needed for notation brevity. From Eq. (13), one has

$$V|_k^- \leq e^{-c_3(T_{k+1}-T_k)} V|_{k-1}^+ \quad (14)$$

during the k^{th} step, that is, $V(x_f)$ is exponentially decreasing during each continuous mode.

The convergence of $\{V|_1^+, V|_2^+, V|_3^+, ...\}$ replies on the continuous-mode convergence rate and the expansiveness of the reset map. From Eq. (12), one has

$$\begin{aligned} \|x_f|_k^+\| =& \|\Delta_{f,x}(T_k^-, x_f|_k^-)\| \\ \leq& \|\Delta_{f,x}(T_k^-, x_f|_k^-) - \Delta_{f,x}(\zeta_k^-, x_f|_k^-)\| \\ &+ \|\Delta_{f,x}(\zeta_k^-, x_f|_k^-) - \Delta_{f,x}(\zeta_k^-, 0)\| \\ &+ \|\Delta_{f,x}(\zeta_k^-, 0)\|. \end{aligned} \quad (15)$$

Suppose that the nominal trajectories are continuously differentiable in t during each continuous mode. Then, it is provable that the reset map $\Delta_{f,x}(t, x_f)$ is continuously differentiable in t and x_f. Therefore, from the previous study [41], there exists a positive number r_1 and Lipschitz constants L_{Δ_t} and L_{Δ_x} such that

$$\|\Delta_{f,x}(T_k^-, x_f|_k^-) - \Delta_{f,x}(\zeta_k^-, x_f|_k^-)\| \leq L_{\Delta_t} \|T_k - \zeta_k\| \quad (16)$$

and

$$\|\Delta_{f,x}(\zeta_k^-, x_f|_k^-) - \Delta_{f,x}(\zeta_k^-, 0)\| \leq L_{\Delta_x} \|x_f|_k^-\| \quad (17)$$

hold for any $x_f(0^+) \in B_{r_1}(0)$.

From our previous study [41], there exists a positive number r_2 and a Lipschitz constant L_{T_x} such that

$$|T_k - \zeta_k| \leq L_{T_x} \|\tilde{x}_f(\zeta_k; T_{k-1}^+, x_f|_{k-1}^+)\| \quad (18)$$

for any $x_f(0^+) \in B_{r_2}(0)$, where $\tilde{x}_f(t; t_0, \lambda_0)$ denotes a solution of $\dot{\tilde{x}}_f = A\tilde{x}_f$ with the initial condition $\tilde{x}_f(t_0) = \lambda_0$, $\forall t > t_0$.

Suppose that $\|\Delta_{f,x}(\zeta_k^-, 0)\| = 0$ is always guaranteed through the proposed trajectory generator to be introduced in Section 6. Then, from Eqs. (15) - (18), one can see that there exist positive constants d and L_d such that $\|x_f|_k^+\|$ is bounded by $\|x_f|_k^-\|$ and $\|\tilde{x}(\zeta_k; T_{k-1}^+, x_f|_{k-1}^+)\|$ as

$$\|x_f|_k^+\| \leq L_d(\|x_f|_k^-\| + \|\tilde{x}_f(\zeta_k; T_{k-1}^+, x_f|_{k-1}^+)\|),$$

where, from Eq. (13), one has

$$\|x_f|_k^-\| \leq \sqrt{\frac{c_2}{c_1}} e^{-\frac{c_3}{2c_2}(T_k - T_{k-1})} \|x_f|_{k-1}^+\|$$

and

$$\|\tilde{x}_f(\zeta_k; T_{k-1}^+, x_f|_{k-1}^+)\| \leq \sqrt{\frac{c_2}{c_1}} e^{-\frac{c_3}{2c_2}(\zeta_k - T_{k-1})} \|x_f|_{k-1}^+\|.$$

Hence, the three equations above yield

$$\|x_f|_k^+\| \leq L_d \sqrt{\frac{c_2}{c_1}} e^{-\frac{c_3}{2c_2}(\zeta_k - T_{k-1})} (1 + e^{-\frac{c_3}{2c_2}(T_k - \zeta_k)}) \|x_f|_{k-1}^+\|. \quad (19)$$

Note that the convergence rate $\frac{c_3}{2c_2}$ in Eq. (19) is directly determined by the PD gains. Thus, from Eqs. (13) and (19), it can be known that $\{V|_1^+, V|_2^+, V|_3^+ ...\}$ will be a strictly decreasing sequence for any $x_f(0^+) \in B_d(0)$, where $d = \min(r_1, r_2)$, if the PD gains are chosen such that A in Eq. (12) is Hurwitz and that the continuous-mode convergence rate is sufficiently fast. Then, the closed-loop tracking error dynamics in Eq. (12) will be locally (exponentially) stable.

6 Middle-Level Trajectory Generation

To effectively connect the high-level planner and low-level controller, this section introduces a novel trajectory generator that, in combination with the proposed state-space planner in Section 3, produces a complete set of nominal trajectories for the full-order dynamic model. The main challenge of synthesizing this trajectory generator is to guarantee that the planned nominal trajectories agree with the CoM and foot trajectories generated by the state space planner as well the closed-loop reset map.

We will use the biped model in the left subfigure of Fig. 1 to illustrate our proposed trajectory generator. For simplicity and without loss of generality, the swing-foot ankle joints are not modeled in this study. As the biped has nine DOFs within a continuous mode and is fully actuated (i.e., $m = n = 9$), the biped can track nine nominal trajectories. Three of these trajectories are chosen as the nominal CoM position trajectories, $p_{\text{CoM}}(t)$, which are generated by the state-space planner in Section 3. The remaining six nominal trajectories are chosen as the nominal swing-foot and trunk position trajectories, denoted as $p_{\text{Sw}}(t) : \mathbb{R}^+ \to \mathbb{R}^3$ and $p_{\text{Tr}}(t) : \mathbb{R}^+ \to \mathbb{R}^3$, respectively, and are generated by the proposed motion generator.

Let $r(\theta)$ and $p(t)$ denote the actual and the nominal trajectories of the control variables, respectively. The trajectory tracking errors can be expressed as

$$h := r(\theta) - p(t) := \begin{bmatrix} r_{\text{H}}(\theta) \\ r_{\text{Tr}}(\theta) \\ r_{\text{Sw}}(\theta) \end{bmatrix} - \begin{bmatrix} p_{\text{CoM}}(t) \\ p_{\text{Tr}}(t) \\ p_{\text{Sw}}(t) \end{bmatrix}, \tag{20}$$

where $r_{\text{H}} := [x_{\text{H}}, y_{\text{H}}, z_{\text{H}}] : \Theta_f \to \Theta_{\text{H}} \subset \mathbb{R}^3$ is the actual, 3D hip position, $r_{\text{Tr}} : \Theta_f \to \Theta_{\text{Tr}} \subset \mathbb{R}^3$ indicates the actual trunk orientation, and $r_{\text{Sw}} : \Theta_f \to \Theta_{\text{Sw}} \subset \mathbb{R}^3$ is the actual, 3D swing-foot position. Note that for simplicity and without loss of generality the hip position is used to approximate the CoM position in this study. Also, the nominal trajectories $p(t)$ in Eq. (20) is planned as non-periodic because uneven terrain walking naturally involves nonperiodic motions. The output functions in Eq. (20) can be exponentially driven to zero during continuous modes using the model-based tracking controller introduced in Section 5.2.

Let $p_k(t) := [p_{\text{CoM}_k}^T(t),\ p_{\text{Sw}_k}^T(t),\ p_{\text{Tr}_k}^T(t)]^T$ be a continuously differentiable function on $t \in \mathbb{R}^+$ that coincides with $p(t)$ during the k^{th} step. The following conditions are enforced in the planning of the nominal swing-foot and trunk trajectories:

(A1) The nominal CoM position trajectories $p_{\text{CoM}_k}(t)$, as well as the $(k+1)^{th}$ nominal swing-foot landing instant ζ_{k+1} and support-foot placement $p_{\text{foot}_{k+1}}$, are provided by the state-space planner in Algorithm 1.

(A2) The nominal trajectories $p(t)$ should respect the discrete reset map in Eq. (11) at $t = \zeta_{k+1}$; i.e., $\Delta_{f,x}(\zeta_{k+1}^-, 0) = 0$ should hold.

(A3) The nominal swing-foot position at the end of the k^{th} step matches the $(k+1)^{\text{th}}$ nominal foot placement, i.e., $p_{\text{Sw}_k}(\zeta_{k+1}) = p_{\text{foot}_{k+1}}$.

(A4) The nominal trunk trajectories satisfy $p_{\text{Tr}_k}(t) = 0,\ \forall t > t_p\ (\zeta_k < t_p < \zeta_{k+1})$, to emulate the upright trunk posture during normal human walking [35, 44].

The conditions (A1)–(A4) are incorporated into the following planning algorithm for generating the nominal walking motions during the k^{th} walking step:

Algorithm 2: Trajectory generator of $p_{\text{Sw}_k}(t)$ and $p_{\text{Tr}_k}(t)$.

min $\|\tilde{v}_{\text{H}_k} - \dot{p}_{\text{CoM}_{k+1}}(\zeta_{k+1})\|$

subject to

(i) $[\tilde{v}_{\text{H}_k}; \tilde{v}_{\text{Sw}_k}; \tilde{v}_{\text{Tr}_k}] := \frac{\partial r}{\partial \theta}(\theta^+)\dot{\theta}^+$, where $[\theta^+; \dot{\theta}^+] = \Delta_f(\theta^-, \dot{\theta}^-)$ with $\theta^- = r^{-1}(p_k(\zeta_{k+1}))$ and $\dot{\theta}^- = (\frac{\partial r}{\partial \theta}(\theta^-))^{-1}\dot{p}_k(\zeta_{k+1})$.

(ii) $\|\tilde{v}_{\text{Sw}_k}\|$ and $\|\tilde{v}_{\text{Tr}_k}\|$ are constrained with boxing bounds.

(iii) $\dot{p}_{\text{Sw}_k}(\zeta_k) = \tilde{v}_{\text{Sw}_{k-1}}$ and $\dot{p}_{\text{Tr}_k}(\zeta_k) = \tilde{v}_{\text{Tr}_{k-1}}$, where $\tilde{v}_{\text{Sw}_{k-1}}$ and $\tilde{v}_{\text{Tr}_{k-1}}$ are provided by the previous-step planner as in (i).

(iv) $p_{\text{Sw}_k}(\zeta_{k+1}) = p_{\text{foot}_{k+1}}$.

(v) $p_{\text{Tr}_k}(t) = 0,\ \forall t > t_p := \lambda(\zeta_{k+1} - \zeta_k) + \zeta_k,\ \lambda \leftarrow \frac{1}{3}$.

Note that the condition (A2) is satisfied when the cost function is minimized to zero and the constraints (i)–(iii) are met in Algorithm 2. As analyzed in Section 5.3, the system in Eq. (12) is proved to be locally exponentially stable when the condition (A2) is strictly satisfied and the closed-loop convergence rate is sufficiently high during each continuous mode. In real-world implementations, minimizing the cost function in Algorithm 2 exactly to zero is challenging given limited computational power. Instead, when the minimal cost is a non-zero finite number, the system in Eq. (12) will be locally stable in the sense of Lyapunov, that is, reliable trajectory tracking with a bounded tracking error is guaranteed.

7 Simulations

This section presents the simulation validation of the proposed framework for both flat and uneven terrain walking. We assume that the legs are much lighter and longer than the trunk. Our model has two legs of 9 kg and 0.7 m each and a trunk of 20 kg and 0.1 m.

The state-space motion planner introduced in Section 3 generates nominal CoM trajectories $p_{\text{CoM}}(t) = [x_{\text{CoM}}(t), y_{\text{CoM}}(t), z_{\text{CoM}}(t)]^T$ and foot placements $p_{\text{foot}}(t)$. Given these nominal trajectories, the full-order trajectory generator in Section 6 plans the nominal swing-foot and trunk trajectories $p_{\text{Sw}}(t)$ and $p_{\text{Tr}}(t)$. To track these nominal

trajectories, the model-based controller introduced in Section 5 is applied with PD gains $K_P = 400 \cdot I_{9\times9}$ and $K_D = 40 \cdot I_{9\times9}$, yielding stable closed-loop poles for continuous modes. To evaluate the closed-loop tracking performance of the hybrid full-order model, the initial CoM state deviations are specified as $p_{\mathrm{H}}(0) - p_{\mathrm{CoM}}(0) = [-0.2, -0.2, -0.2]^T$ m and $\dot{p}_{\mathrm{H}}(0) - \dot{p}_{\mathrm{CoM}}(0) = [-0.2, -0.2, -0.2]^T$ m/s.

7.1 Flat terrain walking

The proposed planning and control framework is first evaluated for simulated flat terrain walking. The CoM phase portraits are illustrated in Fig 3. The black dashed lines show the nominal CoM trajectories generated by the state-space planner. Although both CoM positions and velocities experience large initial tracking errors, the actual CoM trajectories converge to a close neighborhood of the nominal trajectories within 0.5 second. The hip velocity $(\dot{x}_{\mathrm{H}}, \dot{y}_{\mathrm{H}})$ experiences persistent small jumps every time after a foot landing due to the rigid-body impact dynamics. These jumps always have bounded magnitudes since the proposed controller guarantees the stability of the hybrid closed-loop system in Eq. (12) in the sense of Lyapunov. As a result, $(\dot{x}_{\mathrm{H}} - \dot{x}_{\mathrm{CoM}}, \dot{y}_{\mathrm{H}} - \dot{y}_{\mathrm{CoM}})$ will also always be bounded in magnitude after an impact. In addition, if the cost function is minimized to zero and the constraints (i)-(iii) in Algorithm 2 are strictly satisfied, $(\dot{x}_{\mathrm{H}} - \dot{x}_{\mathrm{CoM}}, \dot{y}_{\mathrm{H}} - \dot{y}_{\mathrm{CoM}})$ will exponentially converge to zero; i.e., the hybrid closed-loop system in Eq. (12) becomes exponentially stable.

Figure 4 shows the corresponding trunk and swing-foot position trajectories. As shown in the upper plot, the trunk angle $r_{\mathrm{Tr}} = [r_{\mathrm{Tr}_1}, r_{\mathrm{Tr}_2}, r_{\mathrm{Tr}_3}]^T$ experiences transient divergence from zero upon a foot-landing impact and then quickly converges to zero during the rest of a step. Also, the tracking error divergence caused by landing impacts eventually diminishes.

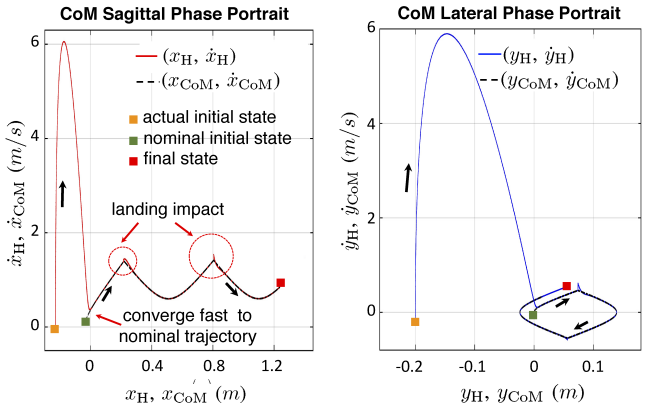

Fig. 3: The CoM sagittal and lateral phase portraits of flat terrain walking. The actual CoM phase portraits (x_{H},$\dot{x}_{\mathrm{H}}$) and (y_{H},$\dot{y}_{\mathrm{H}}$) converge to the nominal phase portraits (x_{CoM},$\dot{x}_{\mathrm{CoM}}$) and (y_{CoM},$\dot{y}_{\mathrm{CoM}}$) under large initial tracking errors. The initial "humps" in the figures represent transient responses to the controller tracking, including acceleration and deceleration phases to chase the desired CoM state.

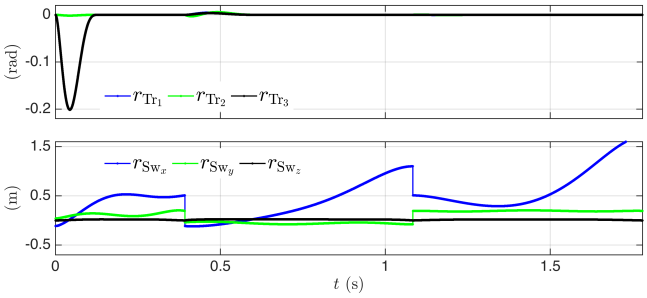

Fig. 4: Trunk angle and swing-foot position trajectories of flat terrain walking.

7.2 Uneven terrain walking

This subsection presents simulation results of bipedal robotic walking over a 3D terrain. The terrain height varies within 15 cm. The nominal support-foot placements p_{foot} are predefined. In this scenario, our simulation generates a sequence of walking stance foot placements with the following terrain height sequence: $0m \rightarrow 0.1m \rightarrow 0.05m \rightarrow 0.14m \rightarrow 0.04m \rightarrow 0.06m \rightarrow 0.1m \rightarrow 0m$. The CoM position and velocity trajectories are shown in Fig. 5. The terrain unevenness is handled by the non-periodic state-space motion planner and reflected in the desired CoM trajectories. The transient tracking errors rapidly decrease to small numbers within the first two steps, which validates the capability of our proposed framework in addressing uneven terrains.

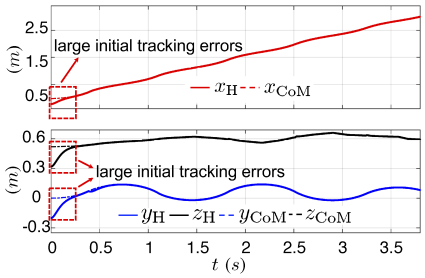

Fig. 5: Uneven terrain walking. The actual CoM trajectories converge sufficiently close to the nominal ones under large initial tracking errors and the varying terrain height.

7.3 Robust walking with state-space re-planning

This subsection shows results of the re-planning strategy in response to external disturbances. In this simulation, an external sagittal disturbance is exerted on the robot's trunk inducing a sudden CoM velocity jump. Multiple strategies can be used to re-plan CoM trajectories as introduced in Subsection 4.2.

High-level re-planning strategies. First, we demonstrate a re-planning strategy that adjusts the next-step keyframe state when an external disturbance causes a positive sagittal velocity jump of 0.2 m/s at $x = 0.7$ m, perturbing the state to be out of the invariant bundle. The re-planning result is shown in Fig. 7(a). The second re-planning strategy is to adjust the CoM surface. Specifically, when the planner detects a sagittal velocity disturbance, the planner re-generates

a new CoM surface for the next step, resulting in a less steep asymptote slope ω in Eq. (5) (see Fig. 6).

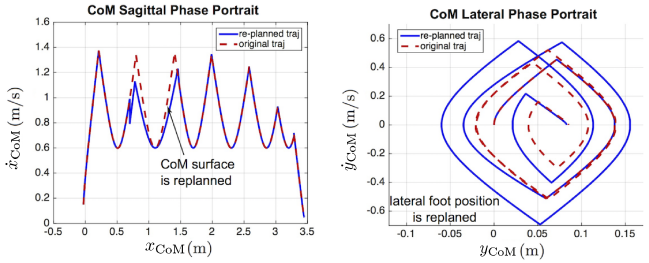

Fig. 6: Robust state-space re-planning via adjusting the desired CoM surface at next walking step. This causes the change of valley-shaped trajectory "opening" profile.

After the state-space planner regenerates new nominal CoM trajectories and foot placements, the trajectory generator in Algorithm 2 re-plans nominal swing-foot and trunk trajectories accordingly, which are tracked by the proposed low-level controller.

Control performance under velocity disturbance during uneven terrain walking. Simulation results are shown in Fig. 7(b). Despite large initial tracking errors and the positive sagittal velocity jump of 0.2 (m/s) at $x = 0.7$ m that perturbs the state out of the invariant bundle, the biped's actual phase portrait still converges to the nominal one sufficiently fast. Compared to Fig. 3, the spikes of actual trajectories in this case become larger due to external disturbance and uneven terrain. Again, these spikes are bounded thanks to (i) the velocity error minimization in Algorithm 2; and (ii) the low-level controller that guarantees satisfactory trajectory tracking of the closed-loop hybrid system.

Note that this simulation explicitly models rough terrain in our motion planner instead of a blind walking without any sense of the terrain profile. As visual sensing techniques for locomotion planning and control become mature, reasoning robustness with accurate or at least partially observable knowledge of the terrain profiles will become more promising means.

For comparison, the same scenario as shown in Fig. 7(b) is simulated again without state-space re-planning of the nominal CoM trajectories and foot placements. It turns out that the walking process fails by the beginning of the third step. This comparison illustrates the effectiveness of our proposed re-planning strategy.

As to the maximum tolerable terrain height variation and disturbance, they depend on the control capability and the walking cycle phase when the disturbance is exerted. This can be solved as an optimization problem and has been investigated in our previous work [32]. More advanced methods on reachability region estimation can be targeted, and we leave it as a future work.

8 Discussions

Explicit robustness quantification regarding discrete dynamics is critical for hybrid systems. Robustness in this study is mainly studied within continuous dynamics. Although we evaluate the controller performance with respect to impact dynamics, we have not proposed any metric to directly characterize the robustness. In future work, we will investigate robustness metrics to quantify the controller performance with respect to impact dynamics. Another future improvement is to account for the impact effect in motion planning to achieve a more coherent planning and control framework.

One of our near-future works aims at incorporating adaptive robust control action into the proposed framework. The trajectory tracking controller design proposed in this paper utilizes input-output linearization, which is sensitive to uncertainties such as external disturbances and modeling errors. To enhance the robustness of trajectory tracking control, previous adaptive robust control [45] will be extended from continuous systems to hybrid systems including legged robots.

We plan to establish a task planning layer above the motion planner layer to achieve more complex locomotion tasks. In that regard, we will use formal methods, such as linear temporal logic [46], to specify high-level abstract tasks and synthesize provably-correct discrete task planners. It will constitute a higher-level decision-making layer. In this case, more advanced feedback re-planning mechanisms can be targeted. In the long-term run, we target a framework of integrated task planning, motion planning, and controller design for enhancing legged locomotion performance.

9 Conclusions

In this study, we propose an integrated planning and control framework to achieve robust and dynamic legged locomotion. The high-level motion planner employs a reduced-order model for task-space trajectory generation. Robustness is formally quantified in the CoM state space by using set theory and incorporated into the robust hybrid automaton. In particular, this non-periodic motion planner is suitable for rough terrain locomotion. Hybrid dynamics are explicitly modeled and used as a basis of the low-level controller design. Synthesized based on full-order dynamic modeling and Lyapunov stability analysis, the low-level controller can achieve provably reliable trajectory tracking. The high-level planner and low-level controller are connected via a middle-level layer of trajectory generation. Although the motion planner and controller in this study are designed for our specific robot configurations, the proposed hierarchical framework and concepts of robust invariant bundles and model-based feedback controller are general to be leveraged to other robotic systems. Flat and uneven terrain locomotion tasks are evaluated in simulations.

References

[1] Chestnutt, J., Lau, M., Cheung, G., Kuffner, J., Hodgins, J., and Kanade, T., 2005. "Footstep planning for the honda asimo humanoid". In Proc. of IEEE In-

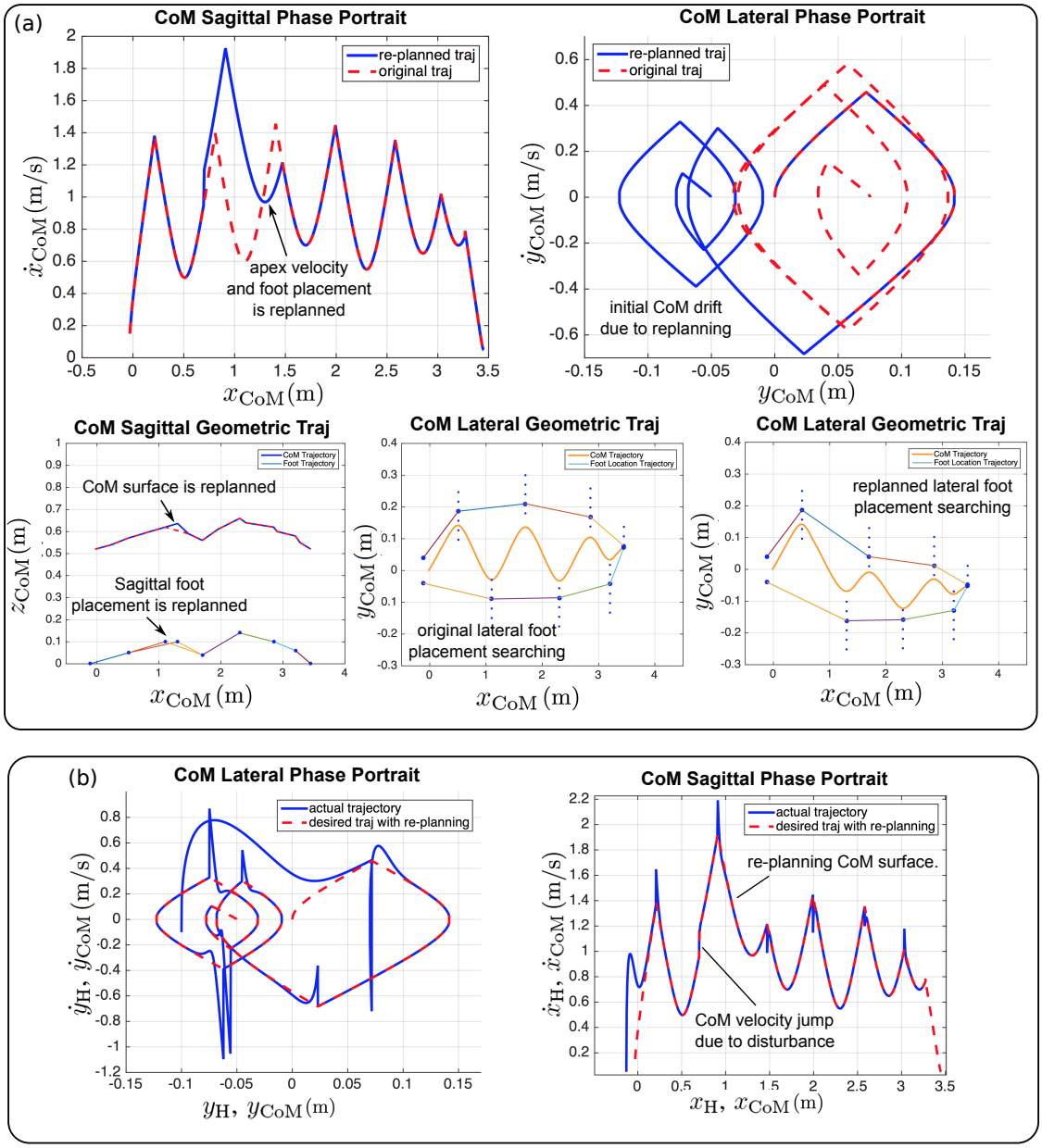

Fig. 7: (a) Robust phase-space re-planning via adjusting next walking step apex velocity and foot placement. Accordingly, all the remaining lateral foot placements are re-searched to synchronize with the new nominal sagittal landing moments. In this particular case, the larger sagittal foot placement after the disturbance leads to a larger lateral foot placement. This causes the initial CoM drift and establishing a new "central" walking line again while moving forward. (b) Tracking results of the re-planned CoM trajectories in (a). Comparing the re-planned nominal trajectories with the actual ones show the high tracking accuracy of the proposed controller. The red and the blue lines are the re-planned nominal trajectories and the actual trajectories, respectively.

ternational Conference on Robotics and Automation, pp. 629–634.

[2] Hauser, K., Bretl, T., Latombe, J.-C., Harada, K., and Wilcox, B., 2008. "Motion planning for legged robots on varied terrain". *The International Journal of Robotics Research,* **27**(11-12), pp. 1325–1349.

[3] Grizzle, J. W., Abba, G., and Plestan, F., 2001. "Asymptotically stable walking for biped robots: Analysis via systems with impulse effects". *IEEE Transactions on Automatic Control,* **46**(1), pp. 51–64.

[4] Ames, A. D., 2014. "Human-inspired control of bipedal walking robots". *IEEE Transactions on Automatic Control,* **59**(5), pp. 1115–1130.

[5] Grizzle, J. W., Chevallereau, C., Sinnet, R. W., and Ames, A. D., 2014. "Models, feedback control, and open problems of 3d bipedal robotic walking". *Automatica,* **50**(8), pp. 1955–1988.

[6] Da, X., and Grizzle, J., 2017. "Combining trajectory optimization, supervised machine learning, and model structure for mitigating the curse of dimensionality in the control of bipedal robots". *arXiv preprint arXiv:1711.02223*.

[7] Nguyen, Q., Agrawal, A., Da, X., Martin, W. C., Geyer, H., Grizzle, J. W., and Sreenath, K., 2017. "Dynamic walking on randomly-varying discrete terrain with one-step preview". In Robotics: Science and Systems.

[8] Feng, S., Whitman, E., Xinjilefu, X., and Atkeson, C. G., 2015. "Optimization-based full body control for the darpa robotics challenge". *Journal of Field Robotics,* **32**(2), pp. 293–312.

[9] Zafar, M., Hutchinson, S., and Theodorou, E. A., 2019. "Hierarchical optimization for whole-body control of wheeled inverted pendulum humanoids". In 2019 International Conference on Robotics and Automation (ICRA), IEEE, pp. 7535–7542.

[10] Zhao, Y., and Sentis, L., 2012. "A three dimensional foot placement planner for locomotion in very rough terrains". In Proc. of IEEE International Conference on Humanoid Robots, pp. 726–733.

[11] Dai, H., Valenzuela, A., and Tedrake, R., 2014. "Whole-body motion planning with centroidal dynamics and full kinematics". In Proc. of IEEE International Conference on Humanoid Robots, pp. 295–302.

[12] Kajita, S., Kanehiro, F., Kaneko, K., Fujiwara, K., Harada, K., Yokoi, K., and Hirukawa, H., 2003. "Biped walking pattern generation by using preview control of zero-moment point". In Proc. of IEEE International Conference on Robotics and Automation, pp. 14–19.

[13] Farshidian, F., Neunert, M., Winkler, A. W., Rey, G., and Buchli, J., 2017. "An efficient optimal planning and control framework for quadrupedal locomotion". In Proc. of IEEE International Conference on Robotics and Automation, pp. 93–100.

[14] Hopkins, M. A., Hong, D. W., and Leonessa, A., 2015. "Compliant locomotion using whole-body control and divergent component of motion tracking". In Proc. of IEEE International Conference on Robotics and Automation, pp. 5726–5733.

[15] Koolen, T., De Boer, T., Rebula, J., Goswami, A., and Pratt, J., 2012. "Capturability-based analysis and control of legged locomotion, part 1: Theory and application to three simple gait models". *The International Journal of Robotics Research,* **31**(9), pp. 1094–1113.

[16] Englsberger, J., Ott, C., and Albu-Schaffer, A., 2015. "Three-dimensional bipedal walking control based on divergent component of motion". *IEEE Transactions on Robotics,* **31**(2), pp. 355–368.

[17] Kajita, S., Kanehiro, F., Kaneko, K., Fujiwara, K., Harada, K., Yokoi, K., and Hirukawa, H., 2003. "Biped walking pattern generation by using preview control of zero-moment point". In IEEE International Conference on Robotics and Automation, pp. 1620–1626.

[18] Koolen, T., Posa, M., and Tedrake, R., 2016. "Balance control using center of mass height variation: Limitations imposed by unilateral contact". In Proc. of IEEE-RAS International Conference on Humanoid Robots, pp. 8–15.

[19] Ramos, O. E., and Hauser, K., 2015. "Generalizations of the capture point to nonlinear center of mass paths and uneven terrain". In Proc. of IEEE-RAS International Conference on Humanoid Robots, pp. 851–858.

[20] Frazzoli, E., 2001. "Robust hybrid control for autonomous vehicle motion planning". PhD thesis, Massachusetts Institute of Technology.

[21] Schouwenaars, T., Mettler, B., Feron, E., and How, J. P., 2003. "Robust motion planning using a maneuver automation with built-in uncertainties". In Proc. of American Control Conference, 2003, pp. 2211–2216.

[22] Majumdar, A., 2013. "Robust online motion planning with reachable sets". Master thesis, Massachusetts Institute of Technology.

[23] Westervelt, E. R., Grizzle, J. W., and Koditschek, D. E., 2003. "Hybrid zero dynamics of planar biped walkers". *IEEE Transactions Automatic Control,* **48**(1), pp. 42–56.

[24] Morris, B., and Grizzle, J. W., 2009. "Hybrid invariant manifolds in systems with impulse effects with application to periodic locomotion in bipedal robots". *IEEE Transactions on Automatic Control,* **54**(8), pp. 1751–1764.

[25] Menini, L., and Tornambè, A., 2001. "Asymptotic tracking of periodic trajectories for a simple mechanical system subject to nonsmooth impacts". *IEEE Transactions on Automatic Control,* **46**(7), pp. 1122–1126.

[26] Galeani, S., Menini, L., and Potini, A., 2011. "Robust trajectory tracking for a class of hybrid systems: An internal model principle approach". *IEEE Transactions on Automatic Control,* **57**(2), pp. 344–359.

[27] Biemond, J. J. B., van de Wouw, N., Heemels, W. P. M. H., and Nijmeijer, H., 2012. "Tracking control for hybrid systems with state-triggered jumps". *IEEE Transactions on Automatic Control,* **58**(4), pp. 876–890.

[28] Forni, F., Teel, A. R., and Zaccarian, L., 2013. "Follow the bouncing ball: Global results on tracking and state estimation with impacts". *IEEE Transactions on Automatic Control,* **58**(6), pp. 1470–1485.

[29] Saccon, A., van de Wouw, N., and Nijmeijer, H., 2014. "Sensitivity analysis of hybrid systems with state jumps with application to trajectory tracking". In Proc. of IEEE Conference on Decision and Control, pp. 3065–3070.

[30] Hurst, J. W., and Rizzi, A. A., 2005. "Physically variable compliance in running". In *Climbing and Walking Robots*. Springer, pp. 123–133.

[31] Pratt, J., Koolen, T., De Boer, T., Rebula, J., Cotton, S., Carff, J., Johnson, M., and Neuhaus, P., 2012. "Capturability-based analysis and control of legged locomotion, part 2: Application to M2V2, a lower-body humanoid". *The International Journal of Robotics Research,* **31**(10), pp. 1117–1133.

[32] Zhao, Y., Fernandez, B., and Sentis, L., 2017. "Robust optimal planning and control of non-periodic bipedal locomotion with a centroidal momentum model". *International Journal of Robotics Research,* **36**(11), September, pp. 1211–1243.

[33] Kuo, A. D., 2002. "Energetics of actively powered locomotion using the simplest walking model". *Journal of biomechanical engineering,* **124**(1), pp. 113–120.

[34] Kuo, A. D., and Zajac, F. E., 1992. "Human standing posture: multi-joint movement strategies based on biomechanical constraints.". *Progress in Brain Re-*

search, **97**, pp. 349–358.

[35] Winter, D. A., 1995. "Human balance and posture control during standing and walking". *Gait & posture,* **3**(4), pp. 193–214.

[36] Zhao, Y., Topcu, U., and Sentis, L., 2016. "High-level reactive planner synthesis for unified legged and armed locomotion in constrained environments". In IEEE Conference on Decision and Control, pp. 6557–6564.

[37] Branicky, M. S., Borkar, V. S., and Mitter, S. K., 1998. "A unified framework for hybrid control: Model and optimal control theory". *IEEE Transactions Automatic Control,* **43**(1), pp. 31–45.

[38] Lygeros, J., Tomlin, C., and Sastry, S., 2008. *Hybrid systems: modeling, analysis and control*. Preprint.

[39] Chevallereau, C., Grizzle, J. W., and Shih, C.-L., 2009. "Asymptotically stable walking of a five-link underactuated 3-D bipedal robot". *IEEE Transactions on Robotics,* **25**(1), pp. 37–50.

[40] Khalil, H. K., 1996. *Nonlinear control*. Prentice Hall.

[41] Gu, Y., Yao, B., and Lee, C. S. G., 2016. "Bipedal gait recharacterization and walking encoding generalization for stable dynamic walking". In Proc. of IEEE International Conference on Robotics and Automation, pp. 1788–1793.

[42] Gu, Y., Yao, B., and Lee, C. G., 2018. "Straight-line contouring control of fully actuated 3-d bipedal robotic walking". In Proc. of American Control Conference, pp. 2108–2113.

[43] Branicky, M. S., 1998. "Multiple Lyapunov functions and other analysis tools for switched and hybrid systems". *IEEE Transaction on Automatic Control,* **43**(4), pp. 475–482.

[44] Herr, H., and Popovic, M., 2008. "Angular momentum in human walking". *Journal of Experimental Biology,* **211**(4), pp. 467–481.

[45] Yao, B., Al-Majed, M., and Tomizuka, M., 1997. "High-performance robust motion control of machine tools: an adaptive robust control approach and comparative experiments". *IEEE/ASME Transactions on Mechatronics,* **2**(2), pp. 63–76.

[46] Liu, J., Ozay, N., Topcu, U., and Murray, R. M., 2013. "Synthesis of reactive switching protocols from temporal logic specifications". *IEEE Transactions on Automatic Control,* **58**(7), pp. 1771–1785.

Appendix A: Tuple notations in Definition 1

To maintain the notation clarity, we remove the subscript 'r' which denotes the "reduced-order" model. The tuple components of the robust hybrid automaton in Definition 1 are defined as

- Q – set of discrete states. $Q \coloneqq \{q_i\}, i = 1, ..., n$;
- $\mathcal{X}$ – set of spaces of continuous states, x_q, $\mathcal{X} = \cup_q \mathcal{X}_q$. $\mathcal{X}_q \coloneqq \{x_q \in \mathbb{R}^{d_q}, q \in Q\}$;
- Σ – system dynamics, $\Sigma = \cup_q \Sigma_q$, each described by vector field $\mathcal{F}_q$, with $\mathcal{F}_q : \mathcal{X}_q \to T_{\mathcal{X}_q} \subset \mathbb{R}^{d_q}$, where $T_{\mathcal{X}_q}$ is the tangent bundle of $\mathcal{X}_q$;
- $\mathcal{W}$ – disturbance input w space, $w \in \mathcal{W} \subseteq \mathbb{R}^{n_{\text{dist}}}$;
- $\mathcal{U}$ – control inputs space $\mathcal{U} \coloneqq \{u_q, q \in Q\}$. $\mathcal{U} = \{u_c\} \cup \{u_d\}$ where u_c, u_d are continuous and discrete control inputs, respectively;
- I – set of allowable initial conditions, $I \coloneqq \{\zeta_0\} \times \{q\} \times \{x_q\}$, $q \in Q$;
- $\mathcal{D}$ – domain, $\mathcal{D}(q) \coloneqq \{x_q\}$;
- $\mathcal{R}$ – recoverability set, $\mathcal{R} \coloneqq \{\mathcal{R}_q, q \in Q\}$;
- $\mathcal{B}$ - invariant set, $\mathcal{B} \coloneqq \{\mathcal{B}_q, q \in Q\}$;
- $\mathcal{E}$ – edges, $\mathcal{E}_{i,j} = \mathcal{E}(q_i, q_j) : Q \times Q$;
- $\mathcal{G}(q_i, q_j)$ – guard, $\mathcal{G}(q_i, q_j) \coloneqq \{G_{q_i},\ q_i \in Q, q_j \in Q\} \subset \mathcal{X}_{q_i}$;
- $\mathcal{T}(q_i, q_j)$ – jump termination set, $\mathcal{T}(q_i, q_j) \coloneqq \{T_{q_j}, q_i \in Q, q_j \in Q\} \subset \mathcal{X}_{q_j}$;

One thing worthy to concern is the well-posedness [20] of phase-space manifolds. Since our phase-space dynamics are piece-wise continuous, the maneuvers are a finite set of primitives with a finite time durations and the well-posedness of phase-space manifolds is guaranteed for our case.

Ye Zhao received the B.S. degree from The Department of Control Science and Engineering, Harbin Institute of Technology in 2011, and his Ph.D. degree in Mechanical Engineering from The University of Texas at Austin in 2016. From 2017 to 2018, he was a postdoctoral fellow in The John A. Paulson School of Engineering and Applied Sciences, Harvard University. Currently, he is an Assistant Professor in The George W. Woodruff School of Mechanical Engineering at Georgia Institute of Technology. He is affiliated with The Institute for Robotics and Intelligent Machines (IRIM). His research interests lie broadly in planning, decision-making, and optimization algorithms of highly agile and contact-rich robots.

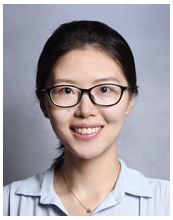

Yan Gu received the B.S. degree in the Department of Mechanical Engineering from Zhejiang University, Hangzhou, China in June 2011 and the Ph.D. degree in the School of Mechanical Engineering from Purdue University, West Lafayette, IN in August 2017. Since September 2017, she has been an Assistant Professor in the Department of Mechanical Engineering at the University of Massachusetts Lowell, Lowell, MA. She is affiliated with the UMass Lowell New England Robotics Validation and Experimentation (NERVE) Center. Her research interests include modeling, planning, and control of hybrid systems with application to legged robotic locomotion.